Electrocoagulation for Treating Petrochemical Wastewater: The Effect of Initial pHs and Voltages

Firman Setiadi [a,b,1], Iqbal Syaichurrozi [a,2,*], Achmad Faizal Ibrahim [a,3], Farhan Fadlurohman Tsaqif [a,4], Muhamad Ariel Satria [a,5], Muhammad Doni Fachriza [a,6], Rahmayetty [a,7]

[a] Department of Chemical Engineering, Engineering Faculty, Universitas Sultan Ageng Tirtayasa, Banten, Indonesia
[b] PT. LOTTE Chemical Indonesia, Banten, Indonesia
[1] firman.setiadi@lotte.net; [2] iqbal_syaichurrozi@untirta.ac.id*; [3] achmadfibrahim@gmail.com; [4] farhantsf30@gmail.com; [5] arilsatria91@gmail.com; [6] 3335220086@untirta.ac.id; [7] rahmayetty@untirta.ac.id
* corresponding author

ARTICLE INFO

Article history
Received October 01, 2025
Revised November 16, 2025
Accepted November 17, 2025

Keywords
Electrocoagulation
Initial pH
Petrochemical wastewater
Voltage

ABSTRACT

Petrochemical wastewater (PW) cannot be discharged directly due to its high chemical oxygen demand (COD), which poses environmental risks. Electrocoagulation (EC) is a promising treatment method capable of reducing COD to meet regulatory standards. This study investigates the influence of initial pH and applied voltage on COD removal during EC treatment of PW. In the first stage, the initial pH was adjusted to 12.25 (control), 9, 7, and 5 at a constant voltage of 10 V. In the second stage, voltages of 5, 10, and 15 V were applied at the previously determined optimum pH. The results showed that an initial pH of 7 produced the highest COD removal (52.96%), outperforming pH 9, 5, and 12.25. The superior performance at neutral pH was attributed to the dominant formation of $Fe(OH)_2$ and $Fe(OH)_3$ coagulants, which effectively destabilize and adsorb organic contaminants. Voltage variation further demonstrated that COD removals of 50.22%, 52.96%, and 55.41% were achieved at 5, 10, and 15 V, respectively, indicating higher removal with increasing voltage. However, increasing voltage also raises operational costs. Economic evaluation revealed that pH 7 and 5 V provided the most cost-effective operation, with the lowest operating cost per $COD_{removed}$ (38.71 IDR/g $COD_{removed}$). Although COD removal at this condition was slightly lower than at higher voltages, the cost savings make it the preferred operating point. These findings highlight key operational parameters for optimizing EC performance and support its sustainable implementation for petrochemical wastewater treatment.

1. Introduction

The petrochemical industry significantly contributes to industrial wastewater generation, producing effluents that contain complex mixtures of organic compounds, oils, heavy metals, and suspended solids. The complexity of petrochemical wastewater arises from its diverse contaminant profile, necessitating effective treatment methods to mitigate adverse environmental impacts and protect public health [1], [2]. Failing to treat these effluents before discharge properly can result in severe ecological degradation and pose risks to local communities, as the contaminated water can disrupt aquatic ecosystems and affect drinking water sources [3], [4]. The Indonesian government has a regulation from the Minister of Environment that stipulates the permissible quality standards for upstream petrochemical industrial wastewater discharged into the environment, namely, chemical oxygen demand (COD) must not exceed 200 mg-O_2/L, biological oxygen demand (BOD) must not exceed 100 mg-O_2/L, TSS must not exceed 150 mg-dry matter/L, and pH levels must between 6-9.

Traditional treatment methods, such as chemical coagulation, biological treatment, and advanced oxidation, have been employed with varying success rates [5], [6]. These approaches, however, often encounter challenges, including extensive chemical requirements, substantial sludge production, and operational complexities [7], [8]. For instance, conventional biological methods may struggle to effectively degrade the high concentrations of toxic contaminants often found in petrochemical wastewater, which can hinder biomass activity and reduce treatment efficacy [4], [9]. Due to these limitations, there is a growing need for more efficient and sustainable alternatives to conventional wastewater treatment processes.

In this context, electrocoagulation (EC) has gained traction as a promising technology for treating petrochemical wastewater. This EC method utilizes an electric current to generate coagulants in situ, thereby reducing the requirement for external chemical additives [9], [10]. The effectiveness of EC lies in its ability to remove various pollutants, such as oils, heavy metals, and suspended solids, while simultaneously minimizing sludge production and simplifying operational processes [11], [12]. Moreover, its operational parameters, particularly initial pH and applied voltage, play a critical role in optimizing treatment performance. The initial pH influences the speciation of coagulant ions and contaminant solubility, while the voltage affects the rate of coagulant generation and energy efficiency [8], [11]. Although electrocoagulation (EC) has been applied to a variety of wastewaters, systematic studies on real petrochemical wastewater with its uniquely complex contaminant profile that simultaneously quantify treatment efficiency, electrode consumption, kinetics, and the trade-offs in operating cost for varying initial pH and voltage remain limited. This study addresses that gap by experimentally evaluating those coupled effects on real petrochemical effluent from Indonesia.

Research into optimizing these parameters is crucial for enhancing the performance of EC systems in petrochemical wastewater treatment. By examining the effects of variables such as initial pH and voltage on treatment outcomes, researchers can further develop strategies to improve the process's efficiency and sustainability. Consequently, this study aims to investigate the influence of these operational parameters on the EC process, providing insights that could lead to better optimization and deployment of this technology in real-world applications, thereby contributing to a more sustainable solution for managing petrochemical wastewater challenges.

2. Research Methodology

2.1. Materials

Petrochemical wastewater (PW) was collected from a petrochemical industry in Cilegon, Indonesia. The fresh petrochemical wastewater (PW) had characteristics shown in Table 1.

Table 1. The Petrochemical Wastewater Characteristic

Parameter	Unit	Value
pH	-	12.25
Color	Pt-Co	7,489.9
TSS (Total Suspended Solids)	mg-dry matter/L	480
Dissolved Iron (Fe)	mg-Fe/L	< 0.09
BOD5	mg-O_2/L	1,706
COD	mg-O_2/L	6,884

The iron electrode plates (mild iron) were obtained from a local market and measured 20 cm × 3.1 cm × 3 mm. The 98% H_2SO_4 solution was obtained from a local market.

2.2. Experimental Set-Up, Design, and Procedures

The detailed experimental setup is presented in Fig. 1. EC pretreatment was conducted in a 1000 mL glass beaker equipped with a magnetic stirrer. The iron electrodes were oven-dried at 105-110°C for two hours before use. As much as 1000 mL of PW was placed in the beaker, and its pH was adjusted using 98% H_2SO_4 to obtain pH values of 12.25 (control, without 98% H_2SO_4 addition), 9, 7, and 5. The electrodes were then immersed in the PW. The active electrode dimension was lengh×width×thickness of 9.5cm×3.1cm×3mm. Meanwhile, the inter-electrode distance was maintained at 5 cm. The cathode and anode were connected to the negative and positive terminals of a DC power supply, respectively. The applied voltages were varied at 15 V, 10 V, and 5 V. The EC

process was carried out under ambient conditions for 80 min with continuous stirring at 500 rpm. The stirrer bar was 3.8 cm long. Every 20 minutes, the liquid temperature and pH were measured using a thermometer and a calibrated digital pH meter. Subsequently, the electrical current was recorded every 20 minutes. A 50 mL sample was then filtered through Whatman No. 42 filter paper, and the filtrate was collected in a 50 mL graduated cylinder and stored in sealed bottles.

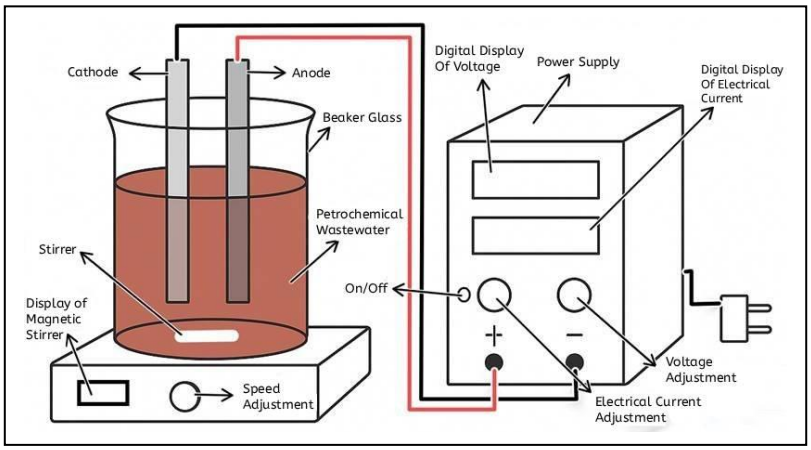

Fig. 1. Laboratory-scale electrocoagulation (EC) set-up

2.3. Analyses

1) pH

The liquid's acidity (pH) was measured with a calibrated digital pH meter.

2) Temperature

The liquid temperature was quantified using a mercury thermometer.

3) Electrical Current

The electrical current was measured by reading the digital display of the power DC supply.

4) COD

The COD concentration was calculated using the dilution factor method. COD analysis was performed using the closed reflux method with spectrophotometry. A 2 mL liquid sample was reacted with COD reagent in a vial, heated in a COD reactor at 150°C for 2 hours, then cooled and measured with a COD meter. The COD of the sample was determined using Equation (1), where c is the COD reading on the COD meter, and f is the dilution factor.

$$\text{COD} = \frac{C}{10} \times f \quad (1)$$

COD removal was obtained from the difference in influent COD and effluent COD values, while the COD removal efficiency was calculated using Equation (2).

$$\text{COD Removal} = \frac{\text{COD}_{influent} - \text{COD}_{effluent}}{\text{COD}_{influent}} \times 100\% \quad (2)$$

5) Electrode weight measurement

Electrode weight was measured to evaluate the rate of electrode material consumption during electrocoagulation. Before the operation, the electrodes were oven-dried at 105-110°C for 2 hours, then weighed on an analytical balance to record their initial mass (W_i). After the process, the electrodes were removed from the reactor, dried, and re-weighed to obtain their final mass (W_f). The difference between these two measurements reflected the amount of electrode material that had dissolved into the solution as a consequence of electrochemical oxidation-reduction reactions.

2.4. Kinetics

The decrease in COD concentration in PW was simulated using empirical first- and second-order kinetic models. The formulas for the two models are shown in Equations (3) and (4).

$$\ln(COD_t) = \ln(COD_0) - k_1 t \quad (3)$$

$$\frac{1}{COD_t} = k_2 t + \frac{1}{COD_0} \quad (4)$$

Where, COD_0 is the initial COD concentration (g/L), COD_t is the COD concentration at time t (g/L), k_1 is the kinetic constant for the first-order model, k_2 is the kinetic constant for the second-order model, t is the operating time (minutes).

In the first-order kinetic model, the graph of the relationship of t vs $\ln(COD_t)$ was made. Then, a linear equation for expressing the relationship of t vs $\ln(COD_t)$. The slope of the equation is k_1. In the second-order kinetic model, the graph of the relationship of t vs $\frac{1}{COD_t}$ was made. Then, a linear equation for expressing the relationship of t vs $\frac{1}{COD_t}$. The slope of the equation is k_2. Microsoft Excel was used in this kinetic analysis.

2.5. Operating Cost

The operational cost in EC needs to be calculated. The operating cost consisted of energy, electrode, and chemical costs. The operating cost (OC, IDR/L) was quantified using Equation (5).

$$OC = A \times C_{energy} + B \times C_{electrode} + C \times C_{chemical} \quad (5)$$

Where, OC is the operating cost (IDR/L), C_{energy} is the energy consumption (Ws/L), $C_{electrode}$ is the electrode consumption (g/L), $C_{chemical}$ is the H_2SO_4 98% chemical consumption (L/L). Unit prices of A, B, and C, based on local prices in Indonesia, are as follows: electrical energy price 27.69×10^{-5} IDR/Ws (watt-second), iron material price 20 IDR/g, and chemical price for technical-grade H_2SO_4 (purity 98% v/v) 15,000 IDR/L. The C_{energy} and $C_{electrode}$ were calculated using Equations (6) and (7), respectively.

$$C_{energy} = \frac{V \times I \times t}{v} \quad (6)$$

$$C_{electrode} = \frac{I \times M_{wFe} \times t}{z \times F \times v} \quad (7)$$

Where, I is the electrical current (A), V is the electrical voltage (V), M_w is the molecular weight of Fe (56 g/mol), z is the number of electron transfer (z=2), F is the Faraday's constant (F=96,485 C/mol), t is the operating time (s), v is the PW volume (L).

Furthermore, the operating cost per g $COD_{removed}$ was calculated using Equation (8).

$$E\left(\frac{IDR}{g\ COD_{removed}}\right) = \frac{OC}{g\ COD_{removed}} \quad (8)$$

3. Results and Discussion

3.1. Effect of Initial pHs at a Voltage of 10 V

The initial pHs play a critical role in determining the performance of the EC process, especially when applied to PW, which generally contains high levels of COD, complex organic compounds, and toxic substances. Variations in pHs can affect the floc formation mechanism, the solubility of metal species produced by the anode, and the stability of colloids in solution [8], [11].

1) Electrode consumption

Table 2. The Changes in Electrode Weight at Various Initial pHs with a Constant Voltage of 10 V

Initial pH	Voltage	Anode Weight (g)			Cathode Weight (g)		
		Before used	*After used*	*Weight loss*	*Before used*	*After used*	*Weight gain*
12.25	10	137.45	133.47	-3.98	137.31	137.43	0.12
9	10	122.40	117.73	-4.67	137.88	137.96	0.08
7	10	126.16	120.52	-5.64	127.12	127.64	0.52
5	10	120.19	115.69	-4.50	127.29	127.33	0.04

Electrode consumption during electrolysis was highly dependent on the initial pH, as shown by the changes in iron electrode mass in Table 2. At pH 7, the anode exhibited the most significant weight loss of 5.64 g, while the cathode simultaneously gained 0.52 g, indicating substantial anode dissolution and cathode precipitation. According to Faraday's law, the rate of anode mass loss is proportional to the electrolysis current and time, with higher current densities accelerating the oxidation of Fe to Fe^{2+} ions [9]. Fe^{2+} then reacts with OH^- to form the coagulant $Fe(OH)_2$, which enhances pollutant destabilization and sludge formation [9]. The significant mass loss at pH 7 indicated that this condition maintained the highest ionic conductivity and current transfer, explaining the superior electrode dissolution and coagulant availability.

At an acidic pH of 5, the anode mass loss was 4.50 g lower than at neutral pH, and the cathode mass gain was minimal at 0.04 g. This phenomenon can be attributed to the fact that under acidic conditions, Fe^{2+} remains more soluble and is less hydrolyzed to $Fe(OH)_2$, thus limiting the formation of stable hydroxide flocs [9], [13]. In addition, the high concentration of H^+ ions competes with Fe^{2+} hydrolysis, increasing corrosion but failing to yield the gelatinous coagulant required for efficient pollutant removal. Under more alkaline conditions of pH 9 and 12.25, the anode losses were 4.67 g and 3.98 g, respectively, lower than at neutral pH, due to the buffering effect that limits Fe dissolution and favors electrode passivation [9]. The changes between anode and cathode masses highlight their different roles, with the anode corroding and becoming porous, while the cathode surface accumulates flocs and sometimes reduces Fe, thus slightly increasing its weight [9]. Overall, the results indicate that pH 7 was the optimal condition, as it promoted the most significant anode dissolution, maximized Fe^{2+} availability, and enhanced coagulant formation, whereas the acidic pH 5 and the highly alkaline pH 9 and 12.25 conditions limited electrode consumption efficiency and treatment performance.

2) pH and Temperature

The pH of the liquid evolved significantly during EC, as shown in Fig. 2. The feeds initially adjusted to pH 5, 7, and 9 showed a consistent upward trend, whereas the original alkaline feed (initial pH 12.25) did not show a consistent change and remained essentially constant. Specifically, the measured pH of the liquid increased from 7.03 to 11.86 at an initial pH of 7, from 5.06 to 10.13 at an initial pH of 5, and from 9.03 to 10.28 at an initial pH of 9 over 80 minutes, while the original alkaline feed remained close to 12.25-12.12 throughout the process. This behavior indicates that cathodic water reduction produces OH^- and H_2 evolution, which accumulate in large amounts and raise the solution pH. Simultaneous dissolution of Fe through the anode process produces Fe^{2+}, which hydrolyzes to $Fe(OH)_2/Fe(OH)_3$, consuming some OH^- but not enough to offset the net OH^- production in most processes [14], [15]. The net OH^- accumulation and moderate temperature increase during electrolysis, therefore, drive an increase in pH in the feed, which starts at or below neutral [16].

The near-constant pH observed in the feed at 12.25 can be attributed to the strong initial alkalinity and the solution's buffering capacity, both from carbonate/bicarbonate and other basic species. When the aqueous phase already contains high OH^-/alkalinity, additional OH^- formation results in only a slight change in the measured pH, and the precipitation/complexation equilibrium tends to stabilize the pH [17]. Conversely, feeds starting at lower pH are more likely to show significant pH increases due to OH^-. From an operational perspective, the pH trajectory is essential because it alters Fe speciation during processing, neutral feeds rapidly evolving towards alkaline conditions favor rapid $Fe(OH)_2/Fe(OH)_3$ formation and promote coagulation, but sustained pH >8–9 risks converting hydroxides to soluble hydroxo anions, e.g., $Fe(OH)_4^-$ and reducing coagulation efficiency [14], [18].

Optimal performance at neutral pH can be explained by Fe(III) speciation. The pC–pH diagrams show that $Fe(OH)_3$ reaches its minimum solubility near pH 7, where it precipitates rapidly and forms dense hydroxide flocs with high surface area, maximizing sweeping coagulation. At lower pH, soluble Fe^{3+} and $Fe(OH)^{2+}$ species dominate, limiting solid hydroxide formation and reducing coagulation efficiency. At higher pH values (>8–9), Fe(III) increasingly forms soluble hydroxo-complexes such as $Fe(OH)_4^-$, which redissolve hydroxide solids and suppress floc formation. This behavior produces the typical bell-shaped relationship between EC performance and pH.

Thus, an initial pH near 7 provides the most favorable balance between hydroxide precipitation and solubility, allowing dissolved Fe^{3+} to convert efficiently into insoluble $Fe(OH)_3$—the primary active coagulant in EC. At low pH, delayed floc formation reduces pollutant destabilization, whereas at high pH, the formation of soluble anionic complexes limits the availability of solid hydroxides. The

minimum-solubility window around pH 7, therefore, yields the strongest coagulation and highest removal efficiency.

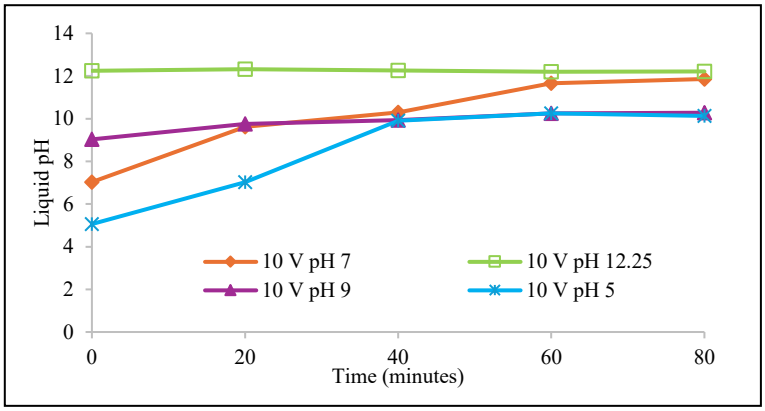

Fig. 2. Liquid pH profiles during the EC process at various initial pHs with a constant voltage of 10 V

The temperature in all processes as seen in Fig. 3. increased steadily for 80 minutes where at pH 7, namely 27 to 78°C, pH 9, namely 30 to 74°C, pH 5, namely 31 to 71.5°C, and pH 12.25, namely 29 to 69°C, which is expected for an electrically driven process where continuous current input converts electrical energy into heat and accelerates the electrochemical reaction [16]. pH 7 achieved the highest temperature because it maintained the highest current, reaching 80 minutes, and because the higher charge transfer resulted in more heating [19]. Furthermore, pH 7 promoted rapid dissolution of the anode Fe and the formation of $Fe(OH)_2/Fe(OH)_3$ flocs, which temporarily increased ionic mobility and conductivity, sustaining higher currents and thus higher temperature rises [17].

The initial alkaline feed, pH 12.25, remained nearly constant at 12.25-12.12 and heated the least, reaching 69°C at the end because its initial alkalinity and high buffering capacity limited the net change in ionic speciation and conductivity during the process, resulting in a minor net increase in current-driven heating [14]. The behavior of pH 5 and 9 intermediates follows the same reasoning: both show the formation of OH^- at the cathode, increasing pH and moderating coagulant production, resulting in intermediate conductivity/current and an increase in the intermediate temperature.

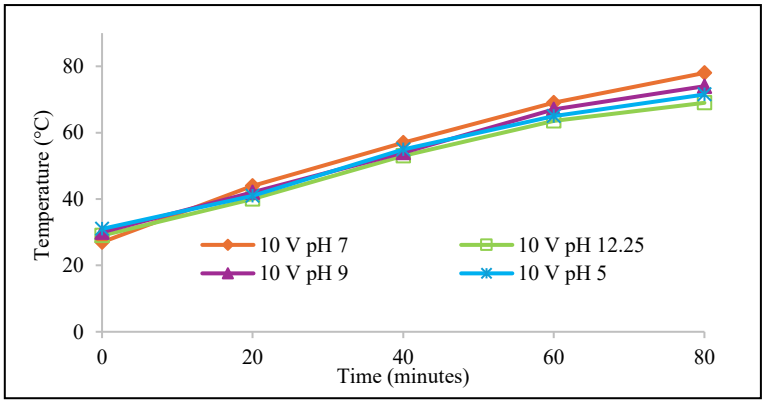

Fig. 3. Temperature profiles during the EC process at various initial pHs with a constant voltage of 10 V

3) COD Removal

The effect of initial pH on COD removal during EC of petrochemical wastewater is a crucial operational factor. The effect of initial pH on COD removal during EC of petrochemical wastewater is shown in Fig. 4. At a constant voltage of 10 V, COD removal efficiencies of 27.92%, 52.96%, 37.00%, and 24.16% were obtained for initial pH values of 5, 7, 9, and 12.25, respectively. These results indicated that neutral conditions, namely pH 7, provided the highest COD removal efficiency. At neutral pH, Fe is predominantly present as $Fe(OH)_2$ and $Fe(OH)_3$, which act as effective coagulants, destabilizing and adsorbing organic pollutants. Under acidic conditions, which is pH 5, basic conditions, namely pH 9, and fundamental conditions, namely pH 12.25, Fe species are primarily present as dissolved ions (Fe^{2+}, Fe^{3+}, $Fe(OH)^+$, $Fe(OH)_3^-$, $Fe(OH)_4^-$), which are less efficient for coagulation [14], [17].

COD removal at pH 9 in this study was 37.00% lower than under neutral conditions, which is consistent with previous reports that, although more hydroxide is formed with increasing alkalinity, excessive precipitation reduces its reactivity and ability to adsorb organic matter [20]. The relatively low efficiency (24.16%) at fundamental conditions, pH 12.25, further supported this observation. The poor performance at acidic pH, pH 5, with an efficiency of 27.92%, was consistent with previous findings that excessive dissolution of Fe ions limited the formation of hydroxide flocs [17].

This observed trend was consistent with previous studies reporting that COD removal increases with increasing solution pH due to increased formation of $Fe(OH)_2$ and $Fe(OH)_3$ coagulants, until reaching a critical range around neutral pH. After that, efficiency decreases as the dissolved hydroxide complexes revert to ionic species [14]. For example, vinasse treated with EC showed the best COD removal at pH 6-7.5, whereas at pH >8, COD removal decreased due to the dominance of dissolved Fe-hydroxo complexes ($Fe(OH)_3$, $Fe(OH)_4^-$). Similarly, [18] emphasized that the removal mechanism is highly dependent on the final pH and the interaction between Fe(II)/Fe(III) with organic matter, which explains the partial removal observed in some cases. Thus, a neutral pH of 7 provided an optimal environment for coagulant formation, resulting in the highest COD removal efficiency, and was therefore selected as the basis for further studies on the effect of applied voltage.

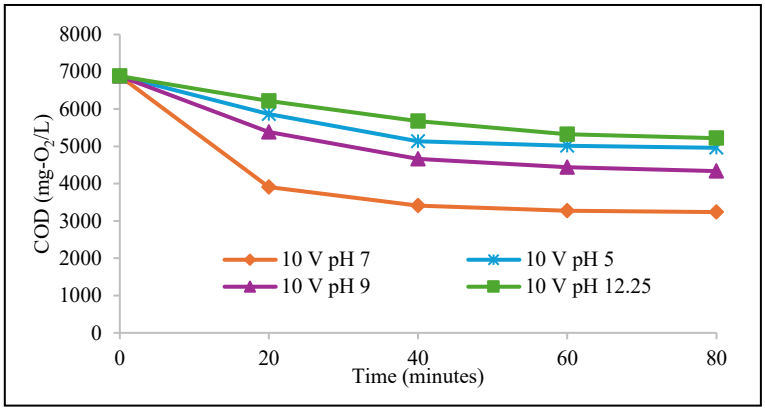

Fig. 4. COD concentration profiles during the EC process at various initial pHs and constant voltage of 10 V

At pH 7, Fe^{2+} generated at the anode was efficiently hydrolyzed to form amorphous $Fe(OH)_2$ and $Fe(OH)_3$. These low-solubility hydroxides readily precipitated into large, reactive flocs that were most effective for sweeping coagulation. At acidic conditions, pH 5, Fe species remained mostly soluble as Fe^{2+}/Fe^{3+}, limiting the formation of solid hydroxides. At alkaline conditions, pH ≥ 9, Fe(III) was further converted into soluble hydroxo-complexes such as $Fe(OH)_4^-$, which re-dissolve or prevent the formation of stable flocs. This pH-dependent speciation explained the bell-shaped efficiency trend and supported why electrode dissolution, coagulant formation, and COD removal all peak at pH 7.

4) Current Profile

Fig.5. shows an increase in electrical current across all initial pH conditions at a fixed cell voltage of 10 V. At 0 min, the current ranged from 5.37 to 5.92 A and increased to 7.34 to 7.89 A after 80 min. The highest current was observed at pH 7 (7.89 A), followed by pH 9 (7.67 A), pH 5 (7.52 A), and the initial alkaline feed pH of 12.25 (7.34 A). This behavior can be interpreted by combining Ohm's law with the solution conductivity that evolves during electrocoagulation, as the cell voltage (V) is kept constant, the electrical resistance (R) decreases, increasing the measured current (I) [16].

The initial increase in current is primarily due to the anodic dissolution of iron, which releases Fe^{2+} and subsequently Fe hydroxyl species, increasing the ionic strength and conductivity of the solution [14], [20]. Simultaneously, electrochemical reactions, including the formation of OH^- at the cathode and a moderate increase in temperature during electrolysis, further reduce the resistivity and thus increase the current [14]. Higher current densities generate more metal ions and OH^-, resulting in more coagulants, which increase conductivity and temporarily increase I for a constant V [20].

The differences in current profiles at various initial pHs were due to Fe speciation and the balance between ion production and ion removal. A neutral pH of 7 produced the highest stable current, consistent with the formation and persistence of dissolved Fe species and the coagulant $Fe(OH)_2/Fe(OH)_3$, which maintained a relatively high ionic content throughout treatment [14]. At very high pHs of 9 and 12.25, or strongly acidic pHs of 5, competing processes (e.g., redissolution to less

conductive hydroxo-anions at very high pH, complexation, or rapid removal of particular ionic species at other pH ranges) can reduce the net conductivity gain and thus result in slightly lower currents [14], [17]. Furthermore, the formation and accumulation of floc/sludge over time can ultimately increase cell resistance by removing ions from the mass and through physical barriers that tend to slow the current increase and bring the system toward a steady state [16].

From an operational perspective, higher currents obtained at pH 7 correlated with better COD removal observed under the same conditions. Increased current, i.e., higher effective charge transfer, and higher local coagulant formation promote the formation of $Fe(OH)_2/Fe(OH)_3$ flocs that remove organic matter [14], [20]. However, studies also warn that increasing current density beyond the optimal value will increase energy consumption, bubble formation, and potential anode passivation, so the operating point must balance removal performance and cost [20].

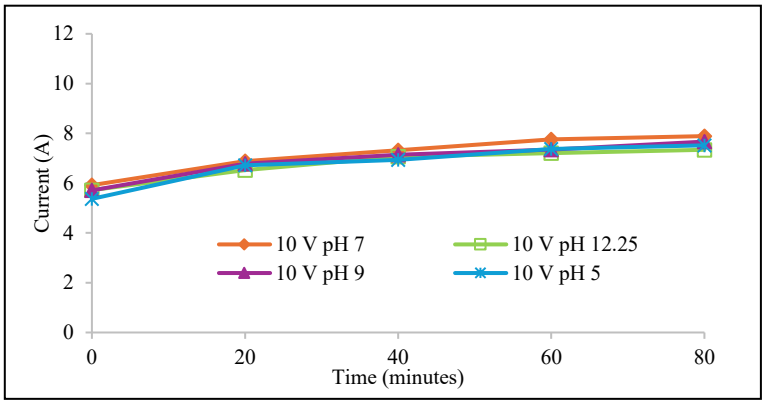

Fig. 5. Electrical current profiles during the EC process at various initial pHs with a constant voltage of 10 V

5) Kinetic analysis

Kinetic analysis using the first and second-order kinetic models was successfully carried out. The 1st-order kinetic model is presented in Fig. 6, and the 2nd-order kinetic model is presented in Fig. 7.

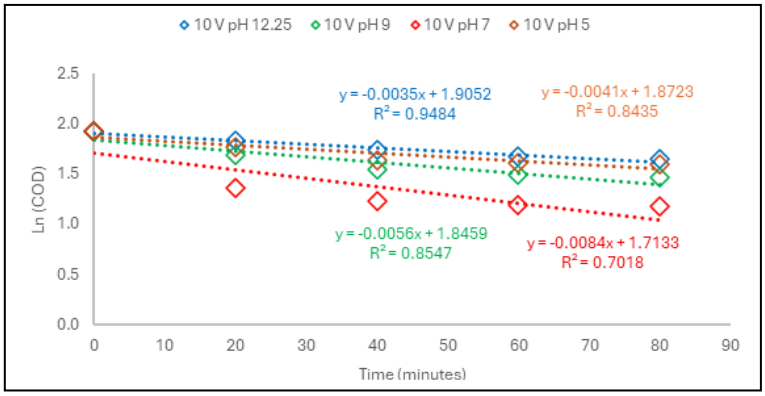

Fig. 6. The 1st-order kinetic model for the EC process at various initial pHs with a constant voltage of 10 V

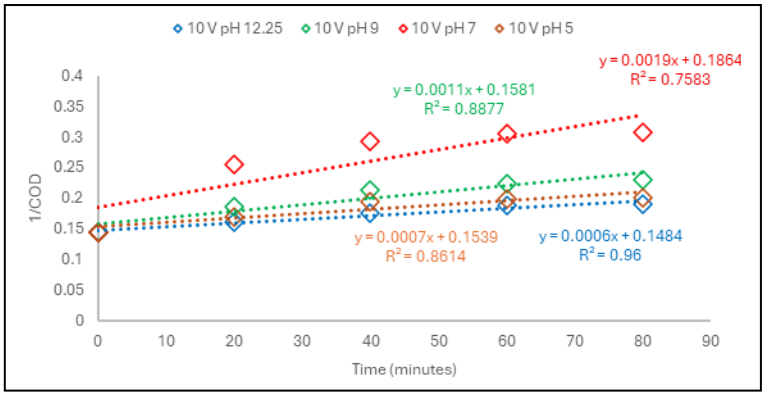

Fig. 7. The 2nd-order kinetic model for the EC process at various initial pHs with a constant voltage of 10 V

Furthermore, the kinetic constant values in both the first-order kinetic model and the second-order kinetic model are shown in Table 3. Based on Fig. 6 and Fig. 7, and Table 3, the decrease in COD concentration during the EC process followed a second-order reaction, as the second-order kinetic model provided a better fit than the first-order model. These results are reasonable, given that electrocoagulation is a complex, heterogeneous process influenced by pH-dependent phenomena, such as the speciation of iron coagulants, the efficiency of floc formation, and the stability of colloidal particles. These factors interact simultaneously during treatment, making simple kinetic assumptions difficult to apply. Therefore, the slightly superior fit of the second-order model under varying pH conditions is more indicative of the multi-component nature of the removal mechanism than evidence of a proper second-order kinetic pathway.

Table 3. The Results of Kinetic Analysis at Various Initial pHs with a Constant Voltage of 10 V

Initial pH	Voltage	First-order		Second-order	
		k_1 (/s)	R^2	k_2 (/(g/L.s))	R^2
12.25	10	0.0035	0.95	0.0006	0.96
9	10	0.0056	0.85	0.0011	0.89
7	10	0.0084	0.70	0.0019	0.76
5	10	0.0041	0.84	0.0007	0.86

According to Table 3, in the second-order kinetic model, the EC process at initial pH of 12.25, 9, 7, and 5 had k_2 kinetic constant of 0.0006, 0.0011, 0.0019, and 0.0007, respectively. It shows that the initial pH of 7 was the most suitable, as it yielded the highest COD removal rate. At pH 7 (neutral), the Fe species predominates as $Fe(OH)_2$ and $Fe(OH)_3$, acting as coagulants. On the other hand, under acidic or alkaline conditions, the Fe species predominates as ions. $Fe(OH)_2$ and $Fe(OH)_3$ coagulants have a higher ability to adsorb COD than Fe ions. Hence, the rate of increase in COD in PW was higher at an initial pH of 7 than at lower or higher pH levels.

Although the second-order model showed slightly higher R^2 values than the first-order model, the improvement was only slight. The second-order model was the better-fitting of the evaluated models, but it did not fully describe the kinetic behavior of the EC process. The modest R^2 values suggested that COD removal during EC was influenced by multiple interacting mechanisms, including Fe dissolution, hydrolysis to $Fe(OH)_2$/$Fe(OH)_3$, floc growth, pollutant adsorption, and mass transfer effects, which were not fully captured by ideal first- or second-order models.

6) Operating cost

The results of the operating cost calculation are presented in Table 4. In the calculation, the authors used the operating time of 40 minutes because after that time, the COD concentrations are not significantly different. According to Table 3, the most efficient EC occurs at an initial pH of 7, with the lowest operating cost per $COD_{removed}$ of 70.07 IDR/g$COD_{removed}$. Therefore, in stage 2, the initial pH of 7 was used with varying electrical voltages.

Table 4. The Results of the Operating Cost Analysis at Various Initial pHs with a Constant Voltage of 10 V and an Operating Time of 40 Minutes

Initial pH	Voltage (V)	Current (A)	t (s)	C_{energy} (Ws/L)	$C_{electrode}$ (g/L)	$C_{chemical}$ (L/L)	OC (IDR/L)	$COD_{removed}$ (g/L)	E (IDR/g $COD_{removed}$)
12.25	10	6.43	2400	154400	4.48	0	132.37	1.66	79.57
9	10	6.54	2400	157040	4.56	6.2×10^{-3}	227.89	2.55	89.47
7	10	6.71	2400	161040	4.67	7.8×10^{-3}	255.45	3.65	70.07
5	10	6.34	2400	152240	4.42	9.9×10^{-3}	279.21	1.92	145.29

As shown in Table 4, the operating cost per liter at pH 7 (255.45 IDR/L) was actually higher than that at pH 12.25 (132.37 IDR/L) and pH 9 (227.89 IDR/L). However, pH 7 achieved substantially higher COD removal (3.65 g/L), resulting in the lowest cost per unit of $COD_{removed}$. This indicates that the advantage of pH seven does not arise from lower operating cost, but from significantly better treatment performance, which compensates for the higher energy and electrode consumption. Therefore, the cost effectiveness at pH 7 reflects an operational balance, with higher removal

efficiency driven by optimal $Fe(OH)_2/Fe(OH)_3$ formation, moderate operating costs, and the lowest normalized cost per $COD_{removed}$. This clarifies that the optimality of pH seven results from the efficiency-cost trade-off rather than solely from the lowest operating expenditure.

3.2. Effect of Voltages at an Initial pH of 7

1) Electrode consumption

Electrode consumption increased substantially with the applied voltage, as shown in Table 5. At 5 V, the anode experienced the lowest weight loss of 0.73 g; at 10 V, 5.64 g; and at 15 V, 6.72 g after 80 minutes of operation. In contrast, the cathode showed a slight weight gain due to deposition of reduced species, with values of 0.09 g, 0.52 g, and 0.21 g at 5 V, 10 V, and 15 V, respectively. This confirms that the anodic dissolution dominates the overall electrode consumption, consistent with Faraday's law of electrolysis. The trend of electrode loss correlated directly with the current density. Voltages of 5, 10, and 15 V resulted in currents of 0.9, 5.92, and 8.42 A at the beginning of the EC process.

Table 5. The Changes in Electrode Weight at Various Voltages with an Initial pH of 7

Initial pH	Voltage	Anode Weight (g)			Cathode Weight (g)		
		Before used	*After used*	*Weight loss*	*Before used*	*After used*	*Weight gain*
7	5	136.9	136.17	-0.73	138.22	138.31	0.09
7	10	127.12	120.52	-5.64	127.12	127.64	0.52
7	15	138.01	131.29	-6.72	121.28	121.49	0.21

2) pH and Temperature

The variations in pH and temperature during the EC process are presented in Fig. 8 and Fig. 9. At 10 V, the pH rose more strongly, increasing from 7.03 at the start to 11.85 after 80 minutes, while at 15 V it rose from 7.07 to 10.45 over the same period. At 5 V, the increase in pH was more moderate, from 7.06 to 8.01 after 80 minutes. This behaviour is explained by competing electrode reactions that scale differently with applied voltage. Increasing voltage increases cathodic water reduction and thus OH^- production, thereby increasing pH. But higher anodic potentials also accelerate two opposing processes that generate acidity or remove OH^-, such as enhanced anodic oxidation of iron to Fe^{3+} (and faster hydrolysis of Fe^{3+}), and increased oxygen evolution reaction (OER, anodic water oxidation) that produces protons (H^+). Both routes counterbalance the cathodic OH^-. At 15 V, the final pH was lower than at 10 V, and this trend can be attributed to competing electrode reactions at high current density. Although OH^- generation at the cathode typically increases pH during EC, the rapid oxidation of water at the anode ($2H_2O \rightarrow O_2 + 4H^+ + 4e^-$) becomes more pronounced at higher voltages. This reaction produces H^+ ions that partially counterbalance the OH^- formed at the cathode, thereby limiting the overall pH increase. As a result, the system exhibited a lower final pH at 15 V than at 10 V, despite the stronger electrical input. Incorporating this effect provided a more accurate interpretation of the pH behavior and aligned with the electrochemical principles governing high-current-density operation. In particular, Fe^{3+} hydrolysis and the formation of hydroxo-iron species release or consume protons or consume OH^-. At a voltage of 10 V, OH^- production at the cathode dominated, and net pH rose strongly. The OH^- production rate exceeded its consumption for coagulant formation, leading to a more pronounced pH increase (from 7.03 to 11.85 within 80 minutes) [19]. At 15 V, the anodic proton-generating reactions and the faster hydrolysis of Fe species became significant enough to neutralize part of the OH-, resulting in a lower net pH increase. At alkaline pH, Fe^{2+} can be converted not only into $Fe(OH)_2$ but also into anionic hydroxo-iron species such as $Fe(OH)_3^-$ and $Fe(OH)_4^-$, thereby limiting further pH increase. This explanation is consistent with previous studies reporting that pH initially increases due to OH^- production, but may stabilize or slightly decrease once OH^- is increasingly consumed in the formation of various hydroxo-iron complexes [14]. The observed lower final pH at 15 V compared with 10 V was consistent with increased anodic oxidation of Fe to Fe^{3+} and OER competing with cathodic OH^- generation at high applied potential. This interpretation also explains why pH sometimes stabilizes or even decreases after an initial rise when voltage and current density are high.

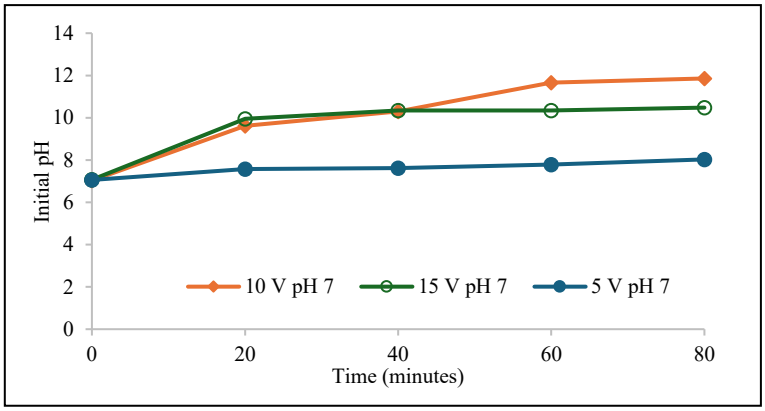

Fig. 8. Liquid pH profiles during the EC process at various voltages with an initial pH of 7

Temperature also showed a strong voltage dependence (Fig. 9). At 15 V, the solution temperature increased steeply from 27°C at 0 min to 89°C at 80 min. At 10 V, it rose from 27°C to 78°C, whereas at 5 V it remained almost constant (from 31°C to 34.5°C). This heating effect is caused by Joule heating as the current increases with voltage. Moderate heating improves mass transfer and accelerates coagulant formation, but excessive heating at 15 V may destabilize flocs and increase energy consumption, thereby reducing process sustainability.

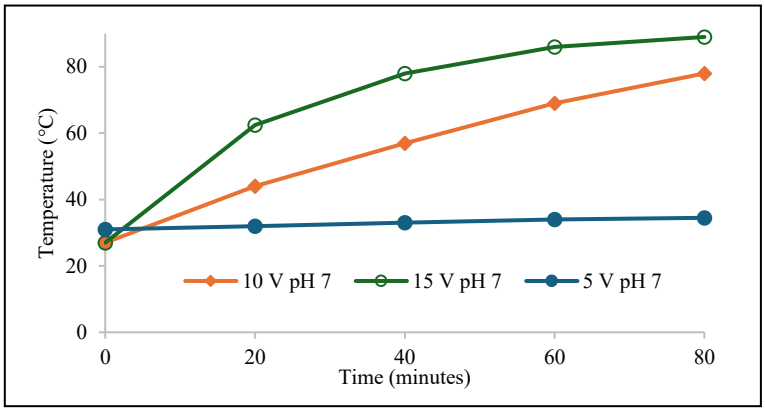

Fig. 9. Temperature profiles during the EC process at various voltages with an initial pH of 7

3) COD Removal

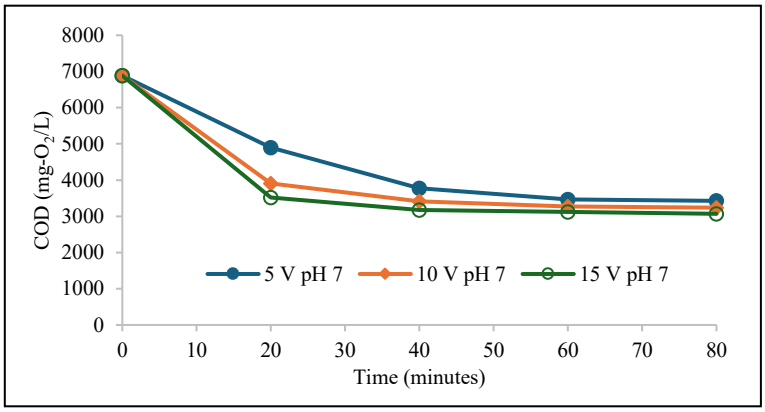

Fig. 10. COD concentration profiles during the EC process at various voltages with an initial pH of 7

The COD concentration profiles at different voltages are shown in Fig. 10. At 15 V, COD decreased from 6884 mg/L to 3069.5 mg/L after 80 minutes, corresponding to a COD removal efficiency of 55.41%. At 10 V, COD was reduced from 6884 mg/L to 3238.5 mg/L (52.96% removal), while at 5 V, the final COD was 3400 mg/L (50.22% removal). The higher current at elevated voltages accelerated anodic dissolution, producing more Fe^{2+}/Fe^{3+} ions that hydrolyzed to $Fe(OH)_2$ and $Fe(OH)_3$, thereby enhancing floc formation [15]. The sharpest COD reduction occurred in the first 20

minutes, where concentrations dropped to around 4000 mg/L at 15 V, indicating rapid destabilization of easily removed organics. Beyond 20 minutes, the COD removal rate slowed, suggesting that more recalcitrant compounds required longer treatment and higher floc availability. Although 15 V achieved the highest COD removal, the difference with 10 V was relatively minor, despite higher electrode and energy consumption. This indicates that excessively high voltages are not favorable from an economic and operational perspective, as they generate unnecessary electrode wear and sludge.

4) Current profile

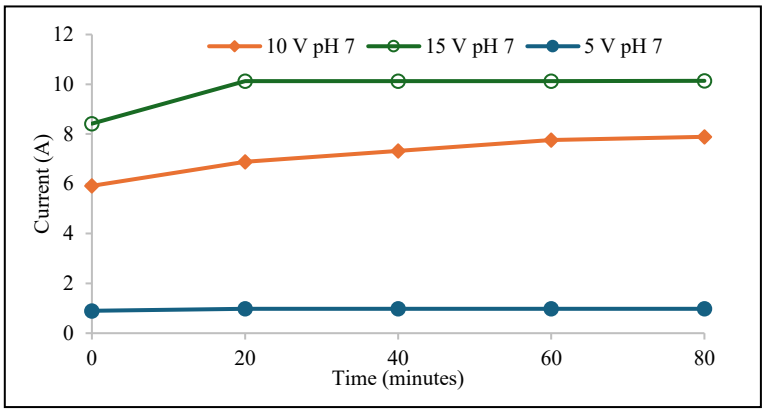

Fig. 11. Electrical current profiles during the EC process at various voltages with an initial pH of 7

The current profiles under different voltages are illustrated in Fig. 11. At 15 V, the current rapidly increased from 8.42 A at the start to about 10.14 A within the first 20 minutes, after which it remained relatively stable until the end of the process. At 10 V, the current rose gradually from 5.92 to 7.89 A, whereas at 5 V it was almost constant at 0.9–1.0 A. This behavior is explained by Equation (9).

$$V = I \times R \tag{9}$$

Resistance (R) changed during the electrocoagulation process. At the beginning, the high concentrations of Fe^{2+} and OH^- ions reduced the solution resistance, leading to a rapid increase in current. As the process progressed, these ions were consumed to form hydroxo-iron species and sludge, thereby increasing resistance and slowing further current growth despite the constant applied voltage [14]. At 15 V, the current stabilized sooner because the resistance increased more rapidly, whereas at 10 V the current continued to rise steadily, reflecting a more balanced balance between ion production and consumption. At 5 V, the driving force for ion generation was too low, so the current remained nearly unchanged throughout the process. Therefore, 10 V represents a balanced condition, combining adequate current for effective pollutant removal with lower energy and electrode consumption compared with 15 V.

5) Kinetic analysis

Kinetic analysis using the first- and second-order kinetic models was successfully carried out. The results for the first-order kinetic model are presented in Fig. 12. Then, the results for the second-order kinetic model are presented in Fig. 13. Furthermore, the kinetic constant values in both the first-order kinetic model and the second-order kinetic model are shown in Table 6.

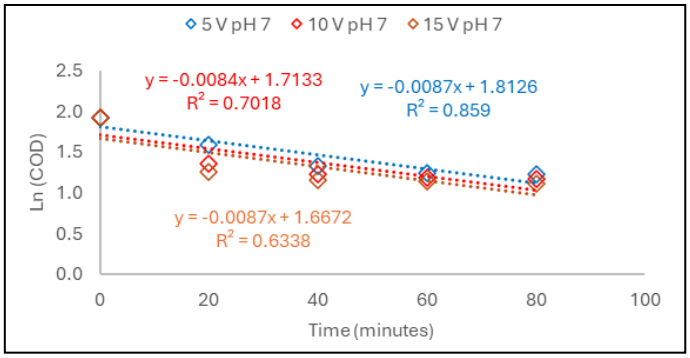

Fig. 12. The results of the 1st-order kinetic model for the EC process at various voltages with an initial pH 7

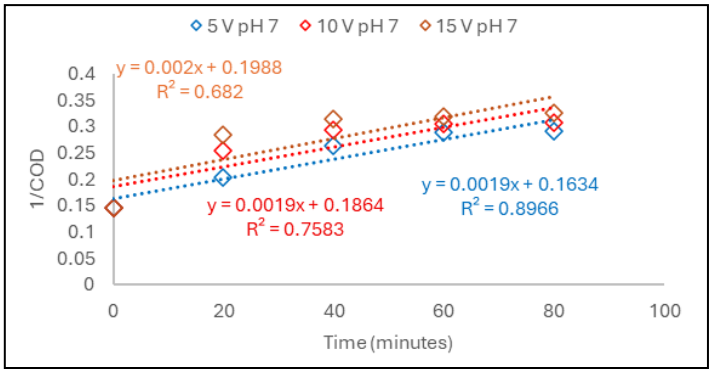

Fig. 13. The results of the 1st-order kinetic model for the EC process at various voltages with an initial pH 7

Table 6. The Results of the Kinetic Analysis at Various Voltages with an Initial pH of 7

Initial pH	Voltage	First-order		Second-order	
		k_1 (/s)	R^2	k_2 (/(g/L.s))	R^2
7	5	0.0087	0.86	0.0019	0.90
7	10	0.0084	0.70	0.0019	0.76
7	15	0.0087	0.63	0.0020	0.68

Based on Fig. 12, Fig. 13, and Table 6, the decrease in COD concentration during the EC process followed a second-order reaction, as the second-order kinetic model provided a better fit than the first-order model. The second-order model consistently produced higher R^2 values, indicating a better fit for all voltage conditions. This is reasonable because electrocoagulation is a complex and heterogeneous process involving pollutant–coagulant interactions, bubble generation, and dynamic changes in the wastewater matrix. Such complexity makes simple kinetic expressions difficult to apply, and the slightly better performance of the second-order model likely reflects the multi-component nature of the removal mechanism rather than an actual second-order reaction behavior.

According to Table 6, in the second-order kinetic model, the EC process at electrical voltages of 5, 10, and 15 V had k_2 kinetic constant of 0.0019, 0.0019, and 0.0020, respectively. It shows that an electrical voltage of 15 V decreases COD more than 5 or 10 V. The higher the voltage, the greater the electrical current supplied, so more $Fe(OH)_2$ and $Fe(OH)_3$ are formed. As a consequence, EC at higher voltages can remove higher COD concentrations. However, the k_2 The value was not significantly different at various voltages (5, 10, and 15 V). Therefore, it is essential to calculate operating costs to determine the optimal EC voltage for treating PW.

6) Operating cost

The operating cost assessment for the EC process is presented in Table 7, using an operating time of 40 minutes because COD reduction becomes relatively stable beyond this duration. While cost analysis identifies 5 V as the most economical condition, a more nuanced interpretation is needed when considering performance, efficiency, and practical applicability. From a performance perspective, 15 V provided the highest COD removal (55.41%) and the fastest reaction kinetics, reflected by the highest second-order rate constant (k_2). This condition maximized treatment effectiveness, but it also resulted in the highest energy consumption of 344.160 Ws/L and electrode dissolution of 6.66 g/L, leading to the highest operating cost of 90.67 IDR/g $COD_{removed}$.

A more balanced option was the 10 V condition, which achieved 52.96% COD removal, only slightly lower than that of the 15 V condition. However, it did so with significantly reduced energy demand and electrode consumption, resulting in a noticeably lower operating cost of 70.07 IDR/g $COD_{removed}$. This makes the 10 V offer strong treatment performance while avoiding the steep cost increase associated with 15 V. In contrast, 5 V emerged as the most economical and sustainable operating point, with the lowest cost of 38.71 IDR/g $COD_{removed}$. Although its COD removal of 50.45% was modestly lower than at 10 and 15 V, the substantial reduction in energy and electrode usage made it far more attractive for scale-up. Overall, although different voltages offer different advantages, 15 V provided the highest removal efficiency, and 10 V offered a reasonable compromise. Based on a trade-off, the results clearly indicate that 5 V is the most optimal operating condition when all key

criteria are considered together. Its substantially lower operating cost, coupled with only marginally lower COD removal compared to higher voltages, makes 5 V the most practical and sustainable choice, particularly for full-scale applications where cost efficiency and long-term operational stability are critical.

Table 7. The Results of the Operating Cost Analysis at Voltages with an Initial pH of 7 and an Operating Time of 40 Minutes

Initial pH	Voltage (V)	Current (A)	t (s)	C_{energy} (Ws/L)	$C_{electrode}$ (g/L)	$C_{chemical}$ (L/L)	OC (IDR/L)	$COD_{removed}$ (g/L)	E (IDR/g $COD_{removed}$)
7	5	0.95	2400	11440	0.66	7.83×10-3	133.84	3.46	38.71
7	10	6.71	2400	161040	4.67	7.83×10-3	255.45	3.65	70.07
7	15	9.56	2400	344160	6.66	7.83×10-3	345.86	3.81	90.67

4. Conclusion

This study evaluated electrocoagulation (EC) for treating petrochemical wastewater (PW) by examining the effects of initial pH and applied voltage. In stage 1, initial pHs of 12.25, 9, 7, and 5 resulted in COD removals of 24.4%, 37.0%, 52.96%, and 27.92%, identifying pH 7 as the optimum. Using this pH in stage 2, voltages of 5, 10, and 15 V achieved COD removals of 50.22%, 52.96%, and 55.41%, respectively. Although higher voltages slightly improved removal efficiency, the economic assessment showed that pH 7 at 5 V provided the most cost-effective operation, yielding the lowest operating cost per $COD_{removed}$ (38.71 IDR/g$COD_{removed}$). This condition is therefore recommended for industrial applications due to its favorable balance between performance and cost. The results also confirm that a neutral pH promotes the formation of $Fe(OH)_3$, the most effective coagulant species produced by iron electrodes, explaining the superior treatment efficiency at pH 7. Overall, the findings highlight the critical role of pH and voltage in optimizing EC performance and support its sustainable implementation for petrochemical wastewater treatment.

Acknowledgment

The authors would like to thank the Direktorat Penelitian dan Pengabdian kepada Masyarakat (DPPM), Direktorat Jenderal Riset dan Pengembangan, Kementerian Pendidikan Tinggi, Sains dan Teknologi - Indonesia, for financial support through the Grant of Penelitian Pasca Sarjana-Penelitian Tesis Magister 2025 with contract numbers 111/C3/DT.05.00/PL/2025 and B/625/UN43.9/PT.00.03/2025 and Universitas Sultan Ageng Tirtayasa (Untirta) - Indonesia for laboratory facility support.

References

[1] A. A. Elamari, A. E. Alshebani, and M. A. M. Saad, "Wastewater treatment from petrochemical industries: the concept and current technologies-a review," *Journal of Marine Science & Environmental Technologies*, vol. 6, no. 1, pp. 20-31, Jun 2020, doi: 10.59743/jmset.v6i1.49.

[2] A. D. M. deMedeiros, C. J. G. d. S. Junior, J. D. P. de Amorim, I. J. B. Durval, A. F. d. S. Costa, and L. A. Sarubbo, "Oily wastewater treatment: methods, challenges, and trends," *Processes*, vol. 10, no. 4, Apr 2022, doi: 10.3390/pr10040743.

[3] S. K. Sharma, N. Thenmani, and R. Kumar, "Hybrid hydrate-based strategy for petrochemical effluent purification and sustainable water management," *Am. Chem. Soc. ES&T Water*, vol. 5, no. 2, pp. 1015-1028, Jan 2025, doi: 10.1021/acsestwater.4c01076.

[4] M. E. Ahmed, A. Mydlarczyk, and A. Al-Haddad, "Efficiency limiting factors of petrochemical wastewater treatment using hybrid biological reactor," *J. Environ. Eng. Landsc. Manag.*, vol. 30, no. 3, Oct 2022, doi: 10.3846/jeelm.2022.17633.

[5] S.Verma, P. Kumar, V. C. Srivastava, and U. Štangar, "Application of advanced oxidation processes (aops) for the treatment of petrochemical industry wastewater," *Advance Industrial Wastewater treatment and Reclamation of Water*, pp. 103-128, Nov 2021, doi: 10.1007/978-3-030-83811-9_6.

[6] X. Wei, M. Kazemi, S. Zhang, and F. A. Wolfe, "Petrochemical wastewater and produced water: Treatment technology and resource recovery," *Water Environ. Res.*, vol. 92, no. 10, pp. 1695-1700, Aug

2020, doi: 10.1002/wer.1424.

[7] T. Paul, I. Janakiraman, K. Pakshirajan, and G. Pugazhenthi, "A review on novel and hybrid/integrated reactor configurations for the removal of recalcitrant organics from petroleum refinery wastewater" *Environ. Qual. Manag.*, vol. 32, no. 1, Aug 2022, doi: 10.1002/tqem.21913.

[8] M. Fedoryak, O. Boruk, S. Boruk, and I. Winkler, "Adsorption of the petrochemical pollutants released at the small vehicle-service facilities on the coal refinery sludge/pyrocarbon compositions," *Inz. Miner.*, vol. 1, no. 1, Dec 2021, doi: 10.29227/IM-2021-01-08.

[9] I. Hajar, Fadarina, M. Zamhari, and S. Yuliati, "Tofu industrial wastewater treatment by electrocoagulation method," *Proc. 4th Forum Res. Sci. Technol.*, Jan 2021, doi: 10.2991/ahe.k.210205.008.

[10] A. Mirshafiee, M. Nourollahi, and A. Shahriary, "Application of electro oxidation process for treating wastewater from petrochemical with mixed metal oxide electrode," *Sci. Rep*., vol. 14, Jan 2024, doi: 10.1038/s41598-024-52201-5.

[11] E. Hartati, L. Hasyyati, D. Agustian, D. Djaenuddin, D. Permana, and H. E. Putra, "Electrocoagulation process for chromium removal in leather tanning effluents," *J. Ecol. Eng.*, vol. 25, no. 4, pp. 1-13, doi: 10.12911/22998993/183554.

[12] M. Apriyanti, S. Sutanto, and L.J. Kusumawardani, "Application of electrocoagulation in soy milk wastewater treatment process with variation of time and voltage," *Helium: J. Sci. Appl. Chem.*, vol. 3, no. 2, Dec 2023, doi: 10.33751/helium.v3i2.8923.

[13] M. Ingelsson, N. Yasri, and E. P. L. Roberts, "Electrode passivation, faradaic efficiency, and performance enhancement strategies in electrocoagulation a review," *Water Res.*, vol. 187, Dec 2020, doi: 10.1016/j.watres.2020.116433.

[14] I. Syaichurrozi, S. Sarto, W. B. Sediawan, and M. Hidayat, "Mechanistic model of electrocoagulation process for treating vinasse waste: effect of initial pH," *J. Environ.. Chem Eng.*, vol. 8, no. 3, Jun 2020, doi: 10.1016/j.jece.2020.103756.

[15] S. G. Segura, M. M. S. G. Eiband, J. V. deMelo, and C. A. M. Huitle, "Electrocoagulation and advanced electrocoagulation processes: A general review about the fundamentals, emerging applications and its association with other technologies," *J. Electroanal. Chem.*, vol. 801, pp. 267-299, Sep 2017, doi: 10.1016/j.jelechem.2017.07.047.

[16] I. Syaichurrozi, S. Sarto, W. B. Sediawan, and M. Hidayat, "Experiment and kinetic analysis of the effect of agitation speed on electrocoagulation process for the treatment of vinasse," *J. Water Process Eng.*, vol. 50, Dec 2020, doi: 10.1016/j.jwpe.2022.103144.

[17] M. Subramaniam and S. Swathi, "Electrocoagulation technique for removing organic and inorganic pollutants (COD) from the various industrial effluents: An overview," *Environ. Eng. Res*., vol. 28, no. 4, Sep 2022, doi: 10.4491/eer.2022.231.

[18] H. A. M. Casillas, D. L. Cocke, J. A. G. Gomes, P. Morkovsky, J. R. Parga, and E. Peterson, "Electrocoagulation:cod removal mechanism," *Separation and Purification Technology*, vol. 56, no. 2, pp. 204-211, Aug 2007, doi: 10.1016/j.seppur.2007.01.031.

[19] Soeprijanto, A. D. Perdani, D. F. Nury, and L. Pudjiastuti, "Treatment of oily bilge water by electrocoagulation process using aluminum electrodes," *AIP Conf. Proc.*, May 2017, doi: 10.1063/1.4982345.

[20] P. Asaithambi, R. Govindarajan, M. B. Yesuf, P. Selvakumar, and E. Alemayehu, "Investigation of direct and alternating current-electrocoagulation process for the treatment of distillery industrial effluent: Studies on operating parameters," *J. Environ. Chem. Eng.*, vol. 9, no. 2, Apr 2021, doi: 10.1016/j.jece.2020.104811.